J. Biomedical Science and Engineering, 2008, 1, 178-181

Enhanced apoptosis and electrostatic acetylcholinesterase activity of abnormally hydrophobic environment in alzheimer's plaques

Rakesh Sharma[1] and Soonjo Kwon[2]

[1]Department of Radiology and Molecular Biology, Columbia University, New York 10032. [2]Department of Biological Engineering, Utah State University, Logan, Utah 84322. Correspondence should be addressed to Rakesh Sharma (rksz2004@yahoo.com).

Received October 6, 2008; revised October 22, 2008; accepted October 22, 2008

ABSTRACT

Alzheimer's disease (AD) is considered a slow neuronal dysfunction process through hypoxia, ischemia and leads to apoptosis mediated senile plaques and neurofibrillary tangles (NFTs). Due to non-invasive approach of plaque characterization, computational techniques based on Brownian dynamics simulation are unique to speculate the electrostatic and kinetic properties of Acetylcholinesterase (AChE). Typically the MRI spectroscopy high choline peak and enzyme specific to Alzheimer's Disease (specificity constant (k_{cat}/K_m) of AChE) appeared associated with apoptosis and hypoxia. A simple display between synergy of cytokines, apoptosis, elevated AChE and choline is postulated as initial events. The events may be distributed heterogeneously within the senile plaques and neurofibrillary tangles (NFTs) of Alzheimer's Disease (AD). The role of decreased brain AChE and synergy was associated with specific Magnetic Resonance Spectroscopic (MRS) pattern profiles in AD. These findings suggest that that the altered AChE and early apoptosis events in AD may be associated with specific MR spectral peak patterns. This study opens the possibility of reduced AChE levels causing high choline and reduced N-acetyl acetate (NAA) neurotransmitter by MRS after initial apoptosis and/or inflammation to make amyloid plaques in the cerebral tissue of Alzheimer's disease (AD) patients. These results can be useful in clinical trials on AD lesions.

Keywords: Alzheimer's Disease, Acetylcholinesterase, Electrostatics, Dielectic effect, Ionic effect, Brownian dynamics, Apoptosis

1. INTRODUCTION

1.1. Alzheimer's Disease

Azheimer's disease (AD) has manifestations of senile plaques and neurofibrillary tangles (NFTs) in the cerebral cortex involving hippocampus of Alzheimer's brains. Many studies have shown that the levels of the reduced ACh neurotransmitter in AD brain had been curiosity in recent past. In this direction, promising success is claimed in drug therapeutic trials based on AChE inhibitors. In AD presumably five neurological cell groups are commonly seen around the cortex rich with AD lesions associated with the low AChE enzyme. Other important problem of AD therapeutics was solved by use of AChE inhibitor higher concentrations such as, tacrine, physostigmine, and BW284C51 to inhibit AChE within AD lesions. Simultaneously, elevated levels of the ACh substrate also inhibit AChE activity. Serotonin, 5-hydroxytryptophan, carboxypeptidase inhibitor, and bacitracin, had been good choice to effectively inhibit cholinesterase activity within plaques and tangles, but fail to alter the AChE activity in normal tissue at standard physiological conditions. The initial stages of amyloid plaque formation are not known if they are the result of metabolic defect leading to pathology. The mechanisms were reviewed by Lu *et al*. 2003 [12]. The process of inflammation in AD was described by Bamberger *et al*. 2002 [5]. There is continuous hunt of biomarkers useful in AD reported by Ankarcrona *et al*. 2002 [3]. However, the sequence of these events remains unknown. There are several reports showing that neurons die partly by apoptosis in the AD brain. Drugs blocking apoptosis could therefore be potentially useful for early prevention of neuronal cell death. Biomarkers for apoptosis should be important tools in the evaluation of drug effects and in the diagnostics of AD. Future strategies are more likely to modify the course of the disease. The most widely accepted hypothesis on the etiopathogenesis of AD proposes that aggregates of beta amyloid (Abeta) form in the brain. Under normal conditions, the predominant amyloid peptide secreted is Abeta(1-40) with about 10-15% being the longer 1-42 form. In AD, there appears to be an increase in the longer more toxic form which is proposed to trigger tau hyperphosphorylation and neural degeneration. Neurotoxicity is thought to be due to altered calcium regulation, mitochondrial damage and/or immune stimulation. One strategy for treating AD is the prevention of Abeta release or the blockade of it neurotoxic activity re-

ported by Lu 2003 [12].

Present paper explains the electrostatics of lowered AChE catalytic activity in AD brain tissue over normal tissue with possibility of the protein-rich deposits associated with the onset of AD. The paper further, illustrates the possibility of reduced AChE associated with high choline and reduced NAA peaks by MRS and initial events triggered by cytokines, apoptosis and inflammation to synthesize amyloid protein as NFT plaques However, the high concentrations of protein-rich deposits in plaques and NFTs such as βAP, heparan and dermatan sulfate proteoglycans, serum amyloid P component, complement factors, and protein kinase C, had been active research over the increased the hydrophobicity of AChE in AD lesions and abnormally reduced dielectric constant reported by Giambarella *et al*. 1997 [9]. The AChE catalysis has been explained as electrostatic steering mechanism where altered dielectric conditions seen by βAP deposition. Possibly, dielectric constant shift in AD tissue also allows Coulombic interactions to permeate longer distances resulting with enhanced enzymatic activity and simultaneously decreased ACh levels. MR spectral pattern of enhanced choline also supports association with decreased ACh levels in AD.

1.2. Acetylcholinesterase

The acetylcholinesterase enzyme (AChE) has 537 amino acid long polypeptide in the postsynaptic neural membranes of central nervous system and neuromuscular junctions by a glycosylphosphatidylinositol linkage. AChE catalyzes the hydrolysis of the acetylcholine (ACh) substrate neurotransmitter at cholinergic synapses. AChE hydrolysis results in the termination of impulse transmission.

The determination of the three-dimensional structure of AChE dimer enzyme comprises 12-stranded mixed β-sheet surrounded by 14 α-helices. These subunits assemble through disulfide linkage and hydrophobic interactions. The enzyme structure shows structural characteristic of AChE as a deep (~20Å), narrow active site making enzyme's catalytic site Ser^{200}, His^{440}, and Glu^{327} at its base. The walls of this entity are lined with 14 highly conserved aromatic amino acids of active site. Positively charged ACh substrate toward the active site caused low-affinity cation-π interactions. Further, amino acid charge distribution over AChE creates an electric field around the enzyme contributing to its enzymatic activity (electrostatic steering mechanism) involving its substrate, ACh [12]. Authors determined that the negative field drives the positively-charged ACh substrate molecule toward the entrance of its active site moiety and increases the catalytic rate of AChE.

1.3. Cytokines, Inflammation, Apoptosis, and Serum AChE Relationship in AD

Inflammatory processes play a role in disease progression and pathology of AD, which involves the deposition of amyloid in the brain and the extensive loss of neurons. Amyloid plaque deposition is accompanied by the association of microglia with the senile plaque, and this interaction stimulates these cells to undergo phenotypic activation and the subsequent expression of proinflammatory cytokines and neurotoxic products [5]. Inflammation has been reported in numerous neurodegenerative disorders such as Parkinson's disease, stroke and Alzheimer's disease (AD). In AD, the inflammatory response is mainly located to the vicinity of amyloid plaques. Cytokines, such as Interleukin-1 (IL-1), Interleukin-6 (IL-6), Tumor Necrosis Factor alpha (TNF-α) and Transforming Growth Factor beta (TGF-β) have been clearly involved in this inflammatory process. Although their expression is induced by the presence of amyloid-beta peptide, these cytokines are also able to promote the accumulation of amyloid beta peptide. Altogether, IL-1, IL-6, TNF-α and TGF-β should be considered as key players of a vicious circle leading to the progression of the disease reported by Cacquevel *et al*., 2004 [6]. Inflammatory stimuli also induce nitric oxide production, resulting in oxygen deficiency (hypoxia) and stimulating adenylate cyclase activity. Under these conditions, the rarte of apoptosis increases. Neuron dysfunction is partly due to apoptosis in the AD brain (**Figure 1**).

2. RESULTS AND DISCUSSION

2.1. Ionic Strength

Computed rate constants of Torpedo californica AChE as model enzyme at various ionic strengths are given in **Figure 2**. These values are compared with experimental bimolecular association constants (k_{cat}/K_m) and enzymatic specificity constants (kcat/Km) of a related *Electrophorus electricus* AChE enzyme as reported by Nolte *et al*., 1980 [14]. Since the association constant considers the binding event of the reaction and the specificity constant describes both binding and subsequent catalytic turnover, k_1 is the theoretical maximum value for the calculated diffusion-controlled rate constant, while k_{cat}/K_m sets the lower limit on these second-order reactions. As seen in **Figure 2**, the calculated rate constants found in this work lie between these two extremes throughout the range of ionic strengths tested. This provides encouraging support for the ionic screening approximations used in this work. Furthermore, the decrease in the rate of AChE catalysis with increasing ionic strength provides strong evidence that an electrostatic steering mechanism plays a role in AChE kinetics. The similarity in the negative slope observed for both association and specificity constants indicates that the ligand binding step of the reaction is dependent upon solvent salt concentration.

2.2. Substrate Radius

To demonstrate the limited accessibility of this enzyme's active site structure, simulations were performed using various substrate radii (**Figure 2**). It is reasonable to predict increased rate constant values with a reduced substrate radius since the probability of a smaller substrate penetrating the active site gorge and reacting with AChE is higher. The results shown in **Figure 3** show this expected

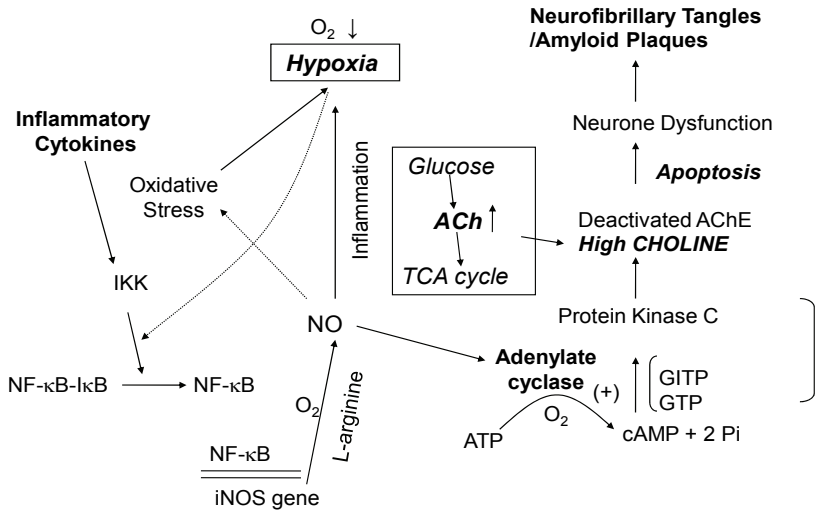

Figure 1. A postulated schematic sketch of the relation among inflammatory cytokines, adenylate cyclase stimulation, AChE and cytotoxicity events in AD. (Solid lines represent stimulation effect and dotted lines represent inhibition effect of different effectors. Abbreviation: IKK; I B kinase kinase, NF- B; nuclear factor B, NF- B-I B; nuclear factor B-inhibitor B complex, NO; nitric oxide, iNOS; inducible nitric oxide synthase, SOD; superoxide dismutase, PKC; protein kinase C, GTP; guanosine triphosphate, GITP; guanylyl imidotriphosphate, ACh; acetylcholine, AChE; acetylcholinesterase enzyme. Possible sequence: Low Oxygen→1. Low ATP (oxidative Phosphorylation); 2. Low Pyruvate (low N-Aceto-Acetate by glycolysis) →High Choline (Reduced AChE). Cytokines trigger adenylate cyclase to inflammation and amyloid protein synthesis ?? (mechanism is unknown).)

Table 1. Effect of Dielectric on Activity of wt AChE. 8000 trajectories were simulated at 300 K, an ionic strength of 5 mM, a solvent density of 996.5 kg/m^3, and a pH of 7.0.

Dielectric constant	Rate Constant $M^{-1}s^{-1}$	Standard Error
78	1.3×10^9	$\pm 0.267 \times 10^9$
60	4.7×10^9	$\pm 0.615 \times 10^9$

trend. These computed rate constants also comparable well with the approximated specificity constant of 4.2 x 10^9 $M^{-1}s^{-1}$ for *Electrophorus electricus* AChE at zero ionic strength [14].

It has been hypothesized that the active site gorge of AChE undergoes conformational fluctuations to allow substrate entry [2]. Further simulation calculations in this work have used a smaller substrate radius (2 Å) than the actual hydrodynamic radius of ACh (4.23 Å) to approximately account for this protein flexibility.

2.3. Reduced Dielectric in Plaques and NFTs

Simulations of the AChE-ACh reaction at both aqueous (ε=78) and hydrophobic (ε=60) conditions demonstrate the substantial effect of the AChE environment on its catalytic activity. The results of this study in **Table 1** reveal that the abnormally low dielectric medium of the enzyme increases its catalytic rate by a factor of 3.6. These results are experimentally supported by Nolte et al. 1980[14], who found a rate constant of 1.6 x 10^9 $M^{-1}s^{-1}$ for *Electrophorus electricus* AChE under similar conditions.

These findings are complemented by the graphical visualization of an intensified electric field near the entrance of the AChE active site gorge in the reduced dielectric environment. This observation can be made by

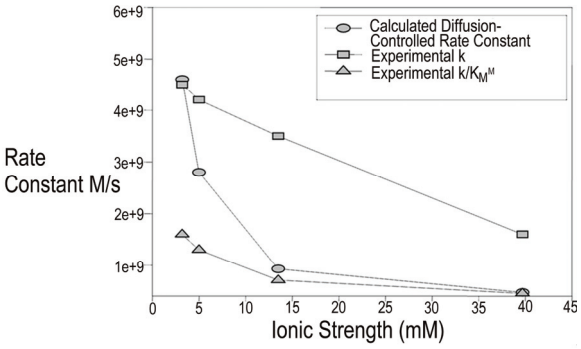

Figure 2. Experimental and Calculated Rate Constants versus Ionic Strength. (Calculations for preliminary ionic strength study used 1000 trajectories at a temperature of 298 K, a dielectric of 78, a solvent density of 997.0 kg/m^3, and a pH of 7.0.)

comparing the electric field contours around the perimeter of AChE at dielectrics of 78 and 60 (**Figure 2**). These contour plots illustrate an electrostatic gradient emerging from the gorge entrance and extending along the enzyme's surface. This effectively enlarges the active site target area, resulting in increased enzyme-substrate association. These electric field calculations along the protein's surface are consistent with the results of Antosiewicz *et al*. 1995b [3], who have suggested that electrostatic steering is limited to operation near the surface of the enzyme. The contour plots found in this work also offer a plausible explanation for the catalytic rate constant enhancement at lower dielectrics and further suggest that electrostatic attraction is an important component of the AChE mechanism and ultimately its physiological role in the human nervous system.

The 3D MP-RAGE at TR/TI/TE=10/250/4 ms, flip an-

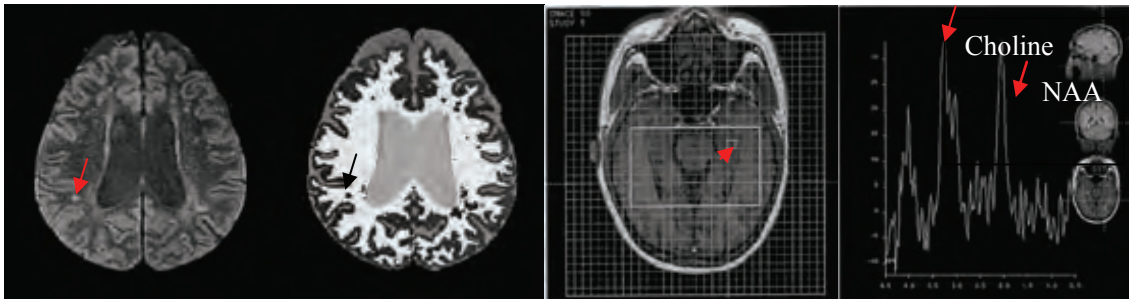

Figure 3. A representative 1.5 Tesla MRI T1 axial image of AD brain (panel A) with post-segmentation (panel B) showin neurofibrillary tangle with arrow.(The scan setting were: 3D MP-RAGE were TR/TI/TE=10/250/4 ms, flip angle 15,1.0 x 1.0 mm^2 resolution, and 1.4 mm thick partitions showing VOI and spectroscopic voxels and selective Choline and NAA spectral peaks from right and left sides to compare metabolites in cortical and ventricular regions (Choline peak on right panel D). For details see reference (Sharma 2005).)

gle 15, 1.0 x 1.0 mm^2 resolution, and 1.4 mm thick partitions in our previous report showed NAA/Cr, NAA/Cho were significantly reduced ($p < 0.02$ and p value < 0.03 respectively) in AD compared with elderly controls due to reductions of NAA after NAA correction in AD. Furthermore, the difference of hippocampal NAA between the groups without atrophy correction (which reflects both NAA and volume changes) was about 40% larger than with correction of atrophy as shown in **Figure 3**. The major elevated peak was choline at 3.00 ppm. These finding suggest a possibility of reduced glycolysis leading to low N-acetyl acetate formation and choline accumulation indirectly reducing TCA cycle to generate enough ATP in localized tissue. Low ATP and oxygen are well understood to lead inflammation and amyloid plaque formation.

3. CONCLUSIONS

Abnormal Magnetic Resonance spectral NAA, choline peak patterns are associated with low AChE enzyme activity in AD with possible enhanced ACh breakdown and surrounding electrostatic field of this enzyme. However, the association of cytokines, apoptosis to lead hypoxia and inflammation in amyloid plaque in AD formation is unclear.

REFERENCES

[1] S. Allison, R. Bacquet, and J. McCammon. (1988) Simulation of the Diffusion-Controlled Reaction between Superoxide and Superoxide Dismutase. II. Detailed Models. Biopolymers, Vol. 27, 251-269.
[2] J. Antosiewicz, J. McCammon, S. Wlodek, and M. Gilson. (1995) Simulation of Charge-Mutant Acetylcholinesterases. Biochemistry, Vol. 34, pg. 4211-4219.
[3] M. Ankarcrona, B. Winblad. (2005) Biomarkers for apoptosis in Alzheimer's disease. Int J Geriatr Psychiatry, 20, 101–105.
[4] J. Antosiewicz, S. Wlodek, J. McCammon. (1996) Acetylcholinesterase: Role of the Enzyme's Charge Distribution in Steering Charged Ligands Toward the Active Site. Biopolymers, Vol. 39, 85-94.
[5] M.E. Bamberger and G. E. Landreth. (2002) Inflammation, Apoptosis, and Alzheimer's Disease. The Neuroscientist, Vol. 8, 276-283.
[6] M. Cacquevel, N. Lebeurrier, S. Cheenne, and D. Vivien. (2004) Cytokines in Neuroinflammation and Alzheimer's Disease. Current Drug Targets, Vol. 5, 529-534.
[7] K. Davis and P. Powchik. (1995) The Lancet, Vol. 345, 625-630.
[8] D. Ermak and J. McCammon. (1978) Brownian Dynamics with Hydrodynamic Interactions.J. Chem. Phys., Vol. 69, 1352-1360.
[9] U. Giambarella, T. Yamatsuji, T. Okamoto, T. Matsui, T. Ikezu. Y. Murayama, M.A. Levine, A. Katz, N. Gautam, and I. Nishimoto. (1997) G protein . complex-mediated apoptosis by familial Alzheimer's disease mutant of APP. The EMBO Journal, Vol. 14, 4897–4907.
[10] T. Golde, S Estus, L Younkin, D Selkoe, and S Younkin. (1992) Processing of the Amyloid Protein Precursor to Potentially Amyloidogenic Derivatives. Science, Vol. 255, 728-730.
[11] J. Hardy and D. Allsop. (1991) Amyloid Deposition as the Central Event in the Aetiology of Alzheimer's Disease.Trends in Pharm. Sci., Vol. 12, pg. 383-388.
[12] D. Lu. (2003) Mechanisms of apoptosis in Alzheimers disease. Journal of Neurochemistry,Vol. 87, 733-41.
[13] R. Nitsch, B. Slack, R. Wurtman and J. Growdon. (1992) Release of Alzheimer Amyloid Precursor Derivatives Stimulated by Activation of Muscarinic Acetylcholine Receptors. Science, Vol. 258, pg. 304-307.
[14] H. Nolte, T. Rosenberry and E. Neumann. (1980) Effective Charge on Acetylcholinesterase Active Sites Determined from the Ionic Strength Dependence of Association Rate Constants with Cationic Ligands. Biochemistry, Vol. 19, 3705-3711.
[15] S. Northrup, S. Allison, and J. McCammon. (1984) Brownian Dynamics Simulation of Diffusion-Influenced Bimolecular Reactions. J. Chem. Phys., Vol. 80, 1517-1524.
[16] F. Rose. (1981) Metabolic Disorders of the Nervous System, Pitman, London, pg. 411.
[17] C. Schätz., C. Geula, and M. Mesulam. (1990) Competitive Substrate Inhibition in the Histochemistry of Cholinesterase Activity in AD. Neurosci. Lttrs., Vol. 117, 56-61.
[18] A. Shafferman, A. Ordentlich, D. Barak, C. Kronman, R. Ber, T. Bino, N. Ariel, R. Osman, and B. Velan. (1994) Electrostatic attraction by surface charge does not contribute to the catalytic efficiency of acetylcholinesterase. EMBO, Vol. 13, 3448-3455.
[19] R. Sharma. (2005) Molecular Imaging by Proton Magentic Resonance Imaging (MRI) and MR Spectroscopic Imaging (MRSI) in Neurodegeneration. Informatica Medica Slovenica, Vol. 10, 35-55.
[20] J. Sussman, M. Harel, F. Frolow, C. Oefner, A. Goldman, L. Toker, and I. Silman. (1991) Atomic Structure of Acetylcholinesterase from *Torpedo californica*: A Prototypic Acetylcholine-Binding Protein. Science, Vol. 253, 872-878.
[21] D. Voet and J. Voet. (1995) Biochemistry, 2nd Edition, John Wiley & Sons, Inc., New York, 317.
[22] D. Voet and J. Voet. (1995) Biochemistry, 2nd Edition, John Wiley & Sons, Inc., New York, 317.